ADVANCED MATERIALS

Energy-Absorbing Hybrid Composites Based on Alternate Carbon-Nanotube and Inorganic Layers

By *Qiang Zhang, Mengqiang Zhao, Yi Liu, Anyuan Cao,* Weizhong Qian, Yunfeng Lu,* and Fei Wei**

Combining materials with distinct structures and dimensions often leads to novel hybrid composites with unexpected properties and unique applications. This idea has been employed in the fabrication of clay mineral–polymer nanocomposites by intercalating polymeric molecules (e.g., epoxy) into layered silicates, and it was later applied to the fabrication of green nanocomposites based on biopolymers and montmorillonite.[1–5] Modulation of the composition and structure of the material on the nanoscale has resulted in improved (and sometimes dramatically different) thermal stability, mechanical stiffness and strength, and barrier properties compared with pure polymers.[2–4] One of the serious challenges, the incompatibility between silicate layers and many polymers, has been overcome to a large extent by using silicates derivatized by appropriate cations, which enhance dispersion in the matrix.[2,3] The key to the successful application of hybrid composites lies in the ability to manipulate the distribution of polymeric molecules among the inorganic layers and the interactions (e.g., chemical bonding) between them.[1,3] However, a number of obstacles remain in the manipulation of the structure of polymer–clay composites at the microscopic scale. For example, polymeric molecules inserted into clay layers by stirring are randomly distributed. After processing, ulvan molecules have been reported to only partially fill the interlayer space between clay layers, and the interlayer distance varied over a wide range.[3] Up to now, a feasible way to control the alignment of molecules during the intercalation has not been found. In addition, the organic matter present in the interlayer space has been considered rigid due to hydrogen bonding with the clay lattice,[3] and it is unlikely to be possible to change the interlayer distance and space once the polymer has been intercalated.

Here, we explored the idea of intercalating vertically aligned carbon nanotubes (CNTs) into naturally existing layered compounds and directly forming a layered hybrid nanocomposite consisting of alternate CNT films and inorganic sheets. Vertically aligned CNT films that were synthesized on planar substrates (e.g., glass, wafer)[6] and shown to have enhanced electrical, optical, and mechanical properties (as opposed to those of random CNTs) have been reported recently.[7] In particular, aligned CNTs exhibit excellent strength and flexibility under mechanical compression, potentially leading to applications as nano- and microscale springs and shock absorbers.[8] We used exfoliated clay compounds as the substrate. Between the clay layers, we intercalated aligned CNT films with a controlled length and density, resulting in a periodic and hierarchical macrostructure with a tailored interlayer distance. The introduction of strong yet flexible CNTs made the resulting composite highly ductile and resilient, in contrast to bare inorganic compounds, which are rigid and brittle; for example, the composite could be compressed to nearly a solid with a volume reduction of up to 90%. The CNT-intercalated composites could be repeatedly compressed at high strains, with an energy absorption capacity nearly 10 times that of the original compounds and four to five times that of conventional plastic foams.

Our experimental method involved small (<3 mm) layered compounds (e.g., vermiculite) that could be impregnated with catalyst seeds in solution and then exfoliated into many thin flat sheets as growth substrates for the in situ intercalation of CNT films (Fig. 1). Impregnation in solutions of $Fe(NO_3)_3$ and $(NH_4)_6Mo_7O_{24}$ followed by calcination in a reducing atmosphere produced Fe/Mo catalyst particles on the surfaces where CNTs then grew, gradually pushing apart the layers. The synthesis thus produced a composite structure consisting of alternating solid inorganic sheets and porous CNT films (Fig. 1, right panel). The composite exhibited an increase in the interlayer spacing from 3 mm in the original vermiculite to 3 cm after CNT growth, with a corresponding volume expansion of more than tenfold, from about 12 to 170 mm^3 (Fig. 2a). Scanning electron microscopy (SEM) images show a periodically layered structure after exfoliation (Fig. 2b), which were then sandwiched by aligned CNTs resulting in an average interlayer distance of 20 μm (Fig. 2c). The as-grown CNTs exhibited uniform length and good alignment, and the vermiculite sheets along the perpendicular direction could be distinguished; a total of about 3000 aligned CNT films were intercalated into one vermiculite block of 3 mm thickness (Fig. 2c). Within a size range for the vermiculite samples of approximately 5–3000 μm, the catalyst impregnation

[*] Prof. A. Cao
Department of Advanced Materials & Nanotechnology
Peking University
Beijing 100871 (PR China)
E-mail: anyuan@pku.edu.cn

Prof. Y. F. Lu
Departments of Chemical Engineering and
Materials Science Engineering
University of California
Los Angeles, CA 90095 (USA)
E-mail: luucla@ucla.edu

Prof. F. Wei, Prof. Y. F. Lu, Dr. Q. Zhang, M. Q. Zhao, Y. Liu,
Prof. W. Z. Qian
Beijing Key Laboratory of Green Chemical Reaction Engineering and
Technology
Department of Chemical Engineering, Tsinghua University
Beijing 100084 (PR China)
E-mail: wf-dce@tsinghua.edu.cn

© 2009 WILEY-VCH Verlag GmbH & Co. KGaA, Weinheim

WILEY InterScience®
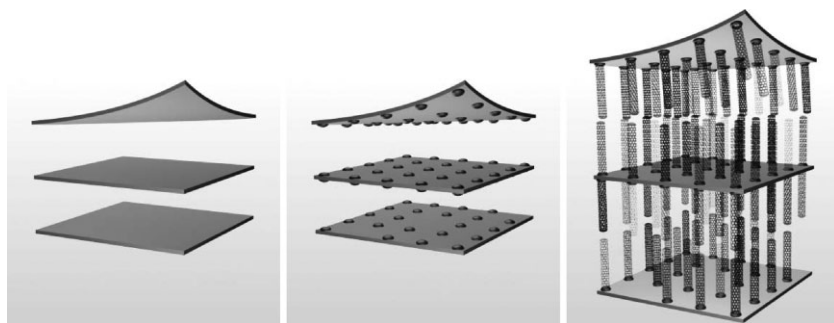DISCOVER SOMETHING GREAT

Figure 1. Illustration of the formation of hybrid composites by intercalating vertically aligned CNT films into layered inorganic compounds, showing stacked layers in the original vermiculite (left panel), catalyst particles adhering to the surface of the layers after impregnation (middle), and aligned CNTs between the layers after the CNT growth process (right).
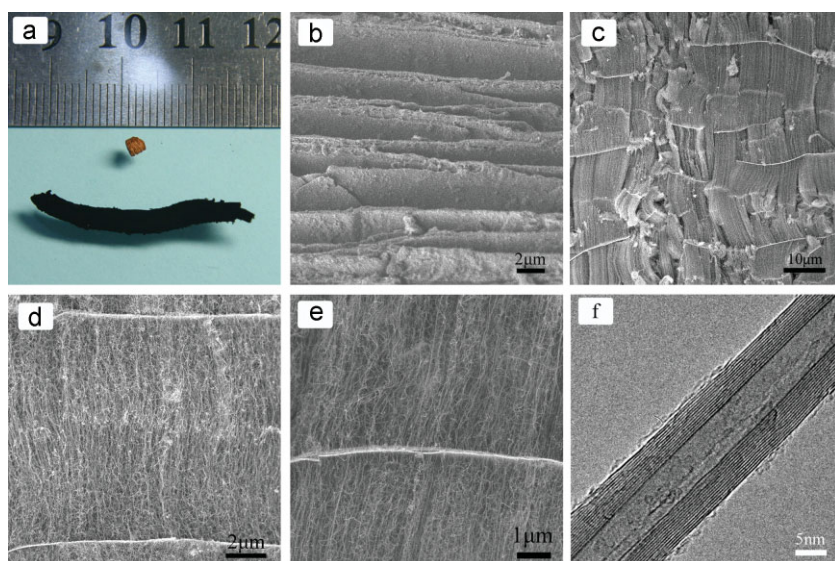

Figure 2. Characterization of hybrid composites: a) Photograph of a fragment of a vermiculite block sample before (arrowed) and after CNT growth. b) SEM image of exfoliated vermiculite before growth. c) SEM image of a vermiculite–CNT composite after intercalation, showing an expanded layered structure comprising alternate CNT films and vermiculite layers; CNT films exhibit uniform length and good alignment. d) SEM image showing an enlarged view of a single interlayer with aligned CNTs and an interlayer distance of 20 μm. e) SEM image showing CNT growth on both sides of a vermiculite layer. f) Transmission electron microscopy image of a multiwalled CNT.

remained for introducing more CNT films by improving the impregnation process and exfoliating the majority of vermiculite layers.

The layer-to-layer distances of the composite, i. e., the length of intercalated CNTs, could be tailored over a wide range (from 200 nm to 100 μm) by varying the time of the chemical vapor deposition (CVD) process. SEM characterization of a composite after a growth time of 30 s revealed short CNTs growing between the vermiculite layers, and the distance between the vermiculite layers increased to about 200 nm (Fig. 3a). This observation indicated that the carbon precursor could infiltrate into the layered vermiculite and the growing CNTs were strong enough to separate the closely packed layers. Continuous growth of the CNTs at a rate of about 20 μm h^{-1} resulted in the interlayer distance gradually increasing from several micrometers to 100 μm within 2.5 h (Fig. S1 and S2, Supporting Information). In a composite intercalated by CNTs with a length of 50 μm (Fig. 3b), the layer-to-layer distance was expanded 50 000 times (from 2 nm in original vermiculite to 100 μm in the composite). We also observed that some compound layers broke into smaller pieces after longer growth periods (more than 10 min), yet the alignment of CNTs was well maintained (Fig. 3b).

This method can be generalized to synthesize a family of CNT composites with similar structures using various catalytic particles (e.g., Ni, Co, and Cu; Fig. S3, Supporting Information), different carbon precursors (e.g., ethylene, propylene, cyclohexane, and liquefied petroleum gas; Fig. S4, Supporting Information), and other layered compounds (e.g., mica and layered alumina; Fig. 3c, d). It was possible to control the density of CNTs intercalating compound layers by using different catalytic materials; CNTs grew at a lower density with Cu than with Fe or Ni as the catalyst (Fig. S3, Supporting Information). In addition, when mica was used as the growth substrate, we observed that the space between adjacent layers was not completely filled with CNTs (Fig. 3c). Such growth inhomogeneity was probably caused by the nonuniform impregnation of catalyst particles on the mica layers, which resulted in the formation (or absence) of CNTs. This demonstrates that a group of layered compounds, such as those studied here, can be exfoliated and intercalated with aligned CNTs to form composites with similar morphology.

A few other reports have described the growth of CNTs on clay substrates, such as montmorillonite.[9] Only random CNTs, however, were produced on separated clay sheets, and the periodic layer-structure of the original substrate was completely lost. Similar agglomerated CNTs were grown on other natural lavas and bentonite.[10] In addition, it was recently reported that
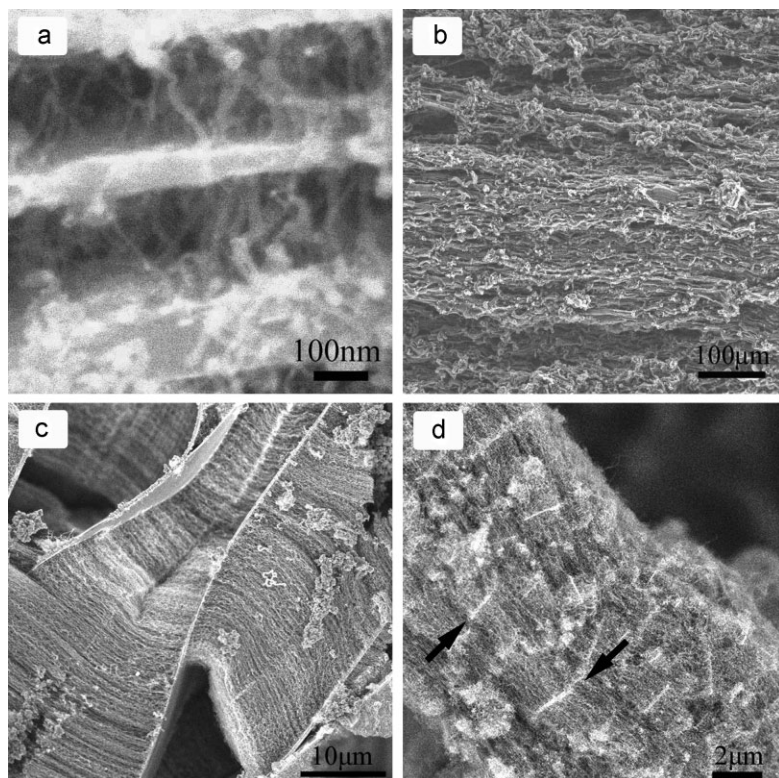
process was uniform, and we observed uniform CNT growth throughout the vermiculite substrate.

Each interlayer consisted of two aligned films that were grown from opposite clay surfaces and joined in the middle (Fig. 2d). This was due to the simultaneous growth of CNTs from both sides of each vermiculite layer (Fig. 2e). Within a single interlayer, CNT growth was uniform and CNT length remained nearly constant. The multiwalled CNTs had an inner diameter of 3–7 nm and an outer diameter of 7–13 nm (Fig. 2f). Since the original vermiculite has an average layer thickness of 20 nm and an interlayer distance of about 2 nm, it was estimated that only a small percentage (~1%) of the layers were intercalated with CNTs. Much potential

Figure 3. SEM images of composites after different growth periods: at the initial stage of growth showing short CNTs between layers (a) and after a growth period of 150 min showing longer CNTs (50 μm) and an interlayer distance of about 100 μm (b). SEM images of composites grown on different substrates: aligned CNTs intercalating a mica substrate (c) and aligned CNTs intercalating a powdered Al_2O_3 substrate, whose layers are indicated by arrows (d).

aligned CNTs can be grown on floating substrates (nanostructured flakes), such as "flying carpets", but the flakes were prepared by roll-to-roll electron-beam evaporation rather than from natural compounds.[11] Compared with those results, our composite maintained an ordered structure in which numerous vertically aligned CNT films were integrated into an intact form with a tunable interlayer distance, which is critical for energy absorption applications. The production of the ordered hierarchical structure was probably due to the improved impregnation process and a separate hydrogen reduction step before CVD, which could enhance the activity of Fe particles and the diffusion of the carbon precursor, resulting in smooth, uniform CNT growth within the entire vermiculite structure.

Compression tests were performed on vermiculite (in natural and exfoliated forms) and CNT–vermiculite composites with a CNT length of 25 and 50 μm (corresponding to interlayer distances of 50 and 100 μm), respectively. At a set compressive stress of 40 MPa, the natural and exfoliated vermiculite samples were broken into powders and the unloading curve dropped immediately to zero (Fig. 4a, inset). Both composite samples were tested repeatedly at several selected stress values, in the range of 4.4 to more than 40 MPa. The stress increased with strain exponentially at higher strain levels (>50%). At the same strain, the compressive strength of the composite with 25-μm-long

CNTs was several times that of the composite with 50-μm-long CNTs (Fig. 4a). Although permanent deformation resulted during initial compression cycles at lower stress levels (e.g., 4.4 and 8.1 MPa) for the composite with 25 μm CNTs, the unloading curve at higher stress values, such as 40.2 MPa, returned to a strain of about 60%, indicating the ability of shape (volume) recovery due to the intercalation of CNTs. The results show that the intercalation of CNTs of appropriate length (e.g., 25 μm) could lead to enhanced mechanical properties. A serious buckling of CNTs in similar aligned films under large compressive strain (e.g., 85%) without structural failure was previously reported.[12]

We compressed vermiculite and composites with different CNT lengths (ranging from 5 to 35 μm) to very high strains, >90% (Fig. 4b), and calculated the energy absorption during compression by integrating the area under the loading curves[13] (Fig. 4c). Vermiculite without CNT intercalation exhibited substantially lower energy absorption (about 16 kJ kg^{-1} at 100 MPa), and its original structure was completely destroyed. For intercalated composites, the energy absorption capacity increased firstly with increasing CNT length until 149 kJ kg^{-1} (for the composite with 25 μm CNTs), but then decreased for the composite with 35 μm CNTs (Fig. 4c, inset). As seen in Figure 4a, longer CNTs (e.g., 50 μm) and larger interlayer separation (100 μm) tended to make the composite soft with a lower compressive strength. Cyclic compression tests on CNT-intercalated composites revealed an excellent reversibility when being compressed at very large strains, 75 to 95% (Fig. 4d). The decrease of energy absorption capacity was within 20% after 20 cycles of compression at 160 MPa, and about 40% of energy was dissipated to the environment in each cycle (Fig. 4d, inset). The maximum value, 149 kJ kg^{-1}, was much higher than that of CNTs in randomly agglomerated forms (70 kJ kg^{-1}) and about 4.5 times that of polystyrene foams (33 kJ kg^{-1}).[12]

We did SEM characterization to further study the compression mechanism. We found that the alignment of CNTs and the formation of the ordered hybrid structure were the most important factors leading to enhanced energy absorption (Fig. S5–S9, Supporting Information). Monitoring the morphology of the composite under different compressive stresses by SEM revealed that the porosity was gradually reduced and the CNTs were highly densified at a stress of 50 MPa or more (Fig. S5, Supporting Information). The composite with 25 μm CNTs and maximum energy absorption maintained CNT alignment and the layered structure after high-pressure (160 MPa) compression (Fig. 5a, b). In contrast, the structure of the composite with longer CNTs (e.g., 50 μm) changed into an entangled form, in which CNTs were not aligned (Fig. 5c, d). These results imply that the enhanced mechanical properties are due to the combination of aligned CNTs with inorganic layers. The process of the compression and release of a CNT-intercalated composite, accompanied by CNT densification and alignment recovery, is illustrated in Figure 5e.
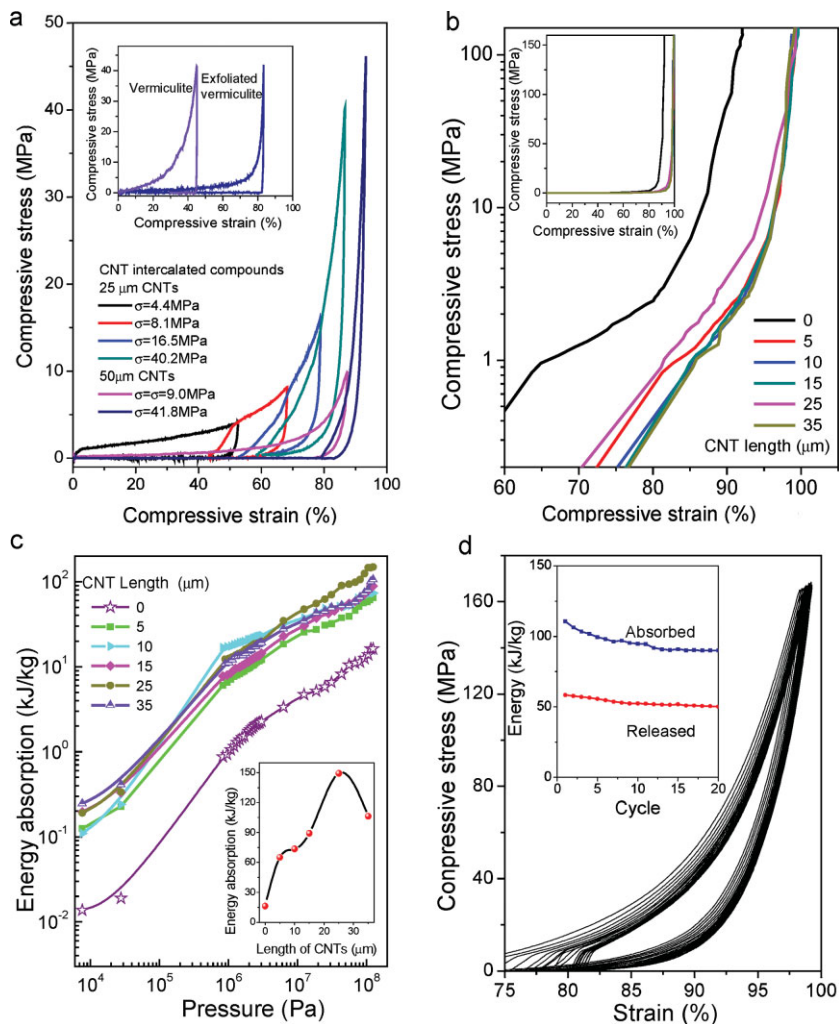
Figure 4. Compression tests and energy absorption of composites. a) Compressive stress–strain curves of vermiculite in original and exfoliated forms (inset) and vermiculite–CNT composites at different set stress values. b) Compressive stress–strain curves of composites with different CNT lengths. c) Energy absorption of vermiculite and composite samples. d) Compressive stress–strain curves of a composite with a CNT length of 25 μm for 20 cycles at a set stress of 160 MPa. Inset, absorbed and released energy of each cycle.

layered natural compounds. The combination of CNTs and inorganic layers in an ordered form has resulted in composites with superior mechanical properties, such as high energy absorption and good cushioning performance. The method is suitable for large-scale production, and the dimension of the composites is easily controllable. More potential applications may arise if the enhanced electrical and optical properties of aligned CNTs, as opposed to random CNTs, were fully exploited. This work also provides a structural platform toward the design of mechanically robust materials that can be used in areas, such as catalysis, separation, ion transportation, energy conversion.

Experimental

The vermiculite and mica used in our experiment were mined in Lingshou, P.R. China. The reactants—$Fe(NO_3)_3 \cdot 9H_2O$, $Ni(NO_3)_2 \cdot 6H_2O$, $Co(NO_3)_2 \cdot 6H_2O$, $Cu(NO_3)_2 \cdot 6H_2O$, $(NH_4)_6Mo_7O_{24} \cdot 4H_2O$, and alumina— were provided by Beijing Yili chemical company.

The exfoliated vermiculite was soaked in a solution of $Fe(NO_3)_3 \cdot 9H_2O$ and $(NH_4)_6Mo_7O_{24} \cdot 4H_2O$ with a Fe/Mo/vermiculite mass ratio of 5:5:90 for 12 h at 80 °C. After filtration, samples were dried at 110 °C for 12 h and calcined at 400 °C for 4 h. The treated vermiculite was placed uniformly in a quartz boat, and inserted into the center of a quartz tube (inner diameter (i.d.): 25 mm, length:1200 mm). The quartz tube was maintained at 650 °C within an atmosphere of argon and hydrogen (10:1) at a flow rate of 600 mL min^{-1}. Then, a mixture of ethylene (80 mL min^{-1}), argon (550 mL min^{-1}) and hydrogen (50 mL min^{-1}) was introduced into the quartz tube for 15 min to allow CNT growth.

$Ni(NO_3)_2 \cdot 6H_2O$, $Co(NO_3)_2 \cdot 6H_2O$, and $Cu(NO_3)_2 \cdot 6H_2O$ were used in place of the $Fe(NO_3)_3 \cdot 9H_2O$ to prepare the Ni/Mo/vermiculite, Co/Mo/vermiculite, and Cu/Mo/vermiculite catalysts, respectively. The M/Mo/vermiculite (M = Ni, Co, Cu) mass ratios were also 5:5:90. After filtration and calcinations, they were put into the CVD reactor for CNT growth with same conditions as in the Fe case. The growth temperature was maintained at 650 °C. The morphology of the as-grown products is shown in Figure S3 in the Supporting Information.

Other carbon sources, such as propylene, cyclohexane, and liquefied petroleum gas, were tested for CNT growth. The flow rate of propylene or liquefied petroleum gas was set at 80 mL min^{-1} by a flowmeter. Cyclohexane was injected into the reactor at a rate of 8.0 mL h^{-1} by a pump. The temperature of the quartz tube reactor was 650 °C. The morphology of the as-grown products grown on the Fe/Mo/vermiculite catalyst from ethylene, propylene, and cyclohexane is shown in Figure S4 in the Supporting Information.

Other catalyst supports, such as lamellar mica and alumina, were also able to function as supports for the Fe/Mo phase. Catalyst preparation and CNT growth were carried out in a manner similar to the above-mentioned procedures. The carbon source was ethylene, and the growth temperature was 650 °C.

The samples were characterized using a JSM 7401F SEM (JEOL Ltd., Tokyo, Japan) operated at 5.0 kV and a JEM 2010 (JEOL Ltd., Tokyo, Japan)
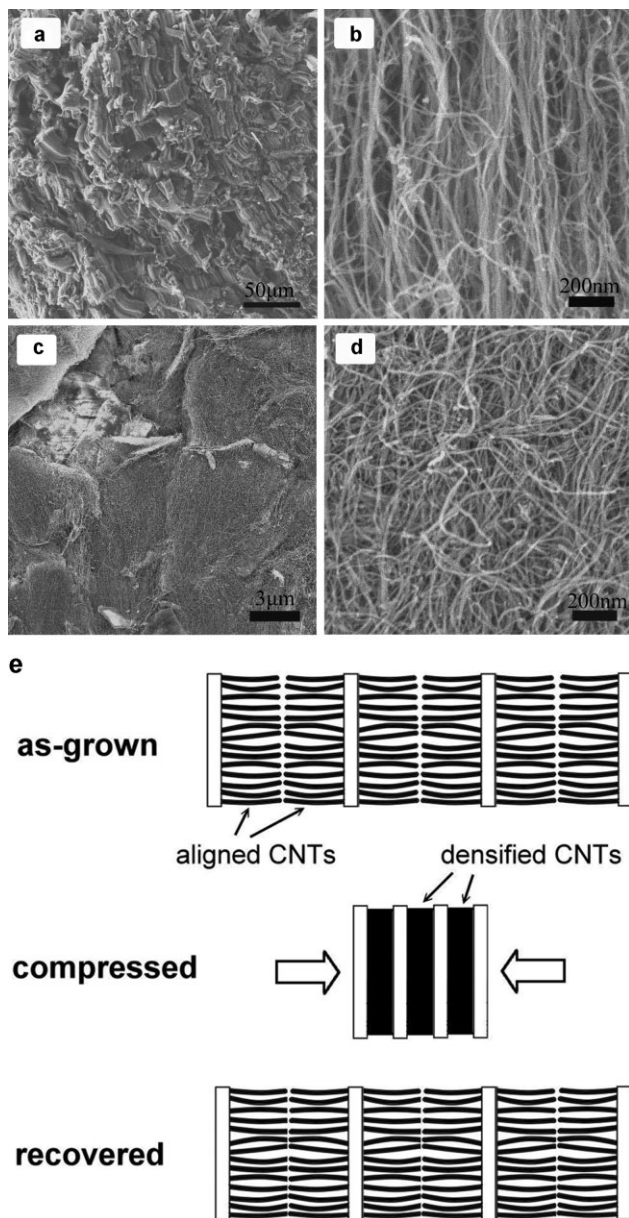
Our results indicate a promising method for the large-scale assembly of CNTs, which is a necessary step toward practical applications. Integration of CNT films along the third dimension (CNT axis), as shown here, promises a maximum utilization of CNT properties and could lead to truly hierarchical, 3D macrostructures. Several attempts to stack multiple layers (less than ten layers) of CNT films in sequence using bottom-up growth and a repetitive synthetic processes have been made, but the methods were not sufficiently efficient to be integrated into a larger scale, and their application are still unclear.[14] Our method could simultaneously assemble thousands of CNT films in a single block of a natural compound.

To summarize, we developed a general synthetic approach to hybrid composites by intercalating vertically aligned CNTs into

ADVANCED MATERIALS

Figure 5. Mechanism study: A composite with 25 μm CNTs after compression, showing the maintainance of the layered structure (a) and CNT alignment (b). A composite with 35 μm CNTs after compression, showing that the layered structure (c) and CNT alignment (d) were disturbed. Illustration of the densification and recovery of aligned CNTs when the composite was compressed and then released (e).

transmission electron microscope operated at 120.0 kV. The cushioning performance was tested using a method similar to that reported by Liu et al. [12]. About 5–10 g of sample was loaded into the cavity of a cylindrical die, and a punch was fixed at the top of the die. Hydrostatic pressure was applied through an oil jack. The displacement and pressure, measured by a micrometer caliper and pressure gauge, were used to calculate the energy absorption density.

[1] G. Lagaly, *Appl. Clay Sci.* **1999**, *15*, 1.

[2] E. P. Giannelis, *Adv. Mater.* **1996**, *8*, 29.

[3] A. L. Laza, M. Jaber, J. Miehé-Brendlé, H. Demais, H. Le Deit, L. Delmotte, L. Vidal, *J. Nanosci. Nanotech.* **2007**, *7*, 3207.

[4] H.-M. Park, M. Misra, L. T. Drzal, A. K. Mohanty, *Biomacromolecules* **2004**, *5*, 2281.

[5] a) P. C. LeBaron, Z. Wang, T. J. Pinnavaia, *Appl. Clay Sci.* **1999**, *15*, 11. b) H. Uyama, M. Kuwabara, T. Tsujimoto, M. Nakano, A. Usuki, S. Kobayashi, *Chem. Mater.* **2003**, *15*, 2492. c) T. Tsujimoto, H. Uyama, S. Kobayashi, *Macromolecules* **2004**, *37*, 1777.

[6] a) W. Z. Li, S. S. Xie, L. X. Qian, B. H. Chang, B. S. Zou, W. Y. Zhou, R. A. Zhao, G. Wang, *Science* **1996**, *274*, 1701. b) Z. F. Ren, Z. P. Huang, J. W. Xu, J. H. Wang, P. Bush, M. P. Siegal, *Science* **1998**, *282*, 1105. c) S. S. Fan, M. G. Chapline, N. R. Franklin, T. W. Tombler, H. J. Dai, *Science* **1999**, *283*, 512. d) R. Andrews, D. Jacques, A. M. Rao, F. Derbyshire, D. Qian, *Chem. Phys. Lett.* **1999**, *303*, 467.

[7] a) Y. Wang, K. Kempa, B. Kimball, J. B. Carlson, G. Benham, W. Z. Li, T. Kempa, J. Rybczynski, A. Herczynski, Z. F. Ren, *Appl. Phys. Lett.* **2004**, *85*, 2607. b) Z. P. Yang, L. Ci, J. A. Bur, S.-Y. Lin, P. M. Ajayan, *Nano Lett.* **2008**, *8*, 446. c) L. Qu, L. Dai, M. Stone, Z. Xia, Z. L. Wang, *Science* **2008**, *322*, 238.

[8] A. Cao, P. L. Dickrell, W. G. Sawyer, M. N. Ghasemi-Nejhad, P. M. Ajayan, *Science* **2005**, *310*, 1307.

[9] a) W. D. Zhang, I. Y. Phang, T. Liu, *Adv. Mater.* **2006**, *18*, 73. b) D. Gournis, M. A. Karakassides, T. Bakas, N. Boukos, D. Petridis, *Carbon* **2002**, *40*, 2641. c) A. Bakandritos, A. Simopoulos, D. Petridis, *Chem. Mater.* **2005**, *17*, 3468.

[10] a) D. S. Su, X. W. Chen, *Angew. Chem. Int. Ed.* **2007**, *46*, 1823. b) D. S. Su, X. W. Chen, X. Liu, J. J. Delgado, A. Schlogl, A. Gajovic, *Adv. Mater.* **2008**, *20*, 3597. c) A. Rinaldi, J. Zhang, J. Mizera, F. Girgsdies, N. Wang, S. B. A. Hamid, R. Schlogl, D. S. Su, *Chem. Commun.* **2008**, 6528.

[11] C. L. Pint, S. T. Pheasant, M. Pasquali, K. E. Coulter, H. K. Schmidt, R. H. Hauge, *Nano Lett.* **2008**, *8*, 1879.

[12] Y. Liu, W. Z. Qian, Q. Zhang, A. Y. Cao, Z. F. Li, W. P. Zhou, Y. Ma, F. Wei, *Nano Lett.* **2008**, *8*, 1323.

[13] a) C. Park, S. R. Nutt, *Mater. Sci. Eng. A* **2000**, *288*, 111. b) J. Banhart, *Prog. Mater. Sci.* **2001**, *46*, 559. c) A. Daoud, M. T. Abou El-khair, M. Abdel-Aziz, P. Rohatgi, *Compos. Sci. Technol.* **2007**, *67*, 1842.

[14] a) X. Li, A. Cao, Y. J. Jung, R. Vajtai, P. M. Ajayan, *Nano Lett.* **2005**, *5*, 1997. b) M. Pinault, V. Pichot, H. Khodja, P. Launois, C. Reynaud, M. Mayne-L'Hermite, *Nano Lett.* **2005**, *5*, 2394.